Article | Received 24 February 2026; Revised 28 May 2026; Accepted 2 June 2026; Published 30 June 2026
https://doi.org/10.55092/aimat20260008

Machine learning-based ion sieve forming strategy: impact on salt lake lithium recovery by fixed beds

Jiangtao Yu[1,*], Zegang Fu[1], Pakiza Ajibek[1], Meng Zhang[2], Weihua Hong[1] and Feng Gao[1,*]

[1] Key Laboratory of Chemical Engineering in South Xinjiang, College of Chemistry and Chemical Engineering, Tarim University, Alar 843300, China
[2] State Key Laboratory of Heavy Oil Processing, College of Chemical Engineering and Environment, China University of Petroleum-Beijing, Beijing 102249, China

* Correspondence authors; E-mails: 120250077@taru.edu.cn (J.Y.); gaofeng137@tju.edu.cn (F.G.).

1. Supplementary figures

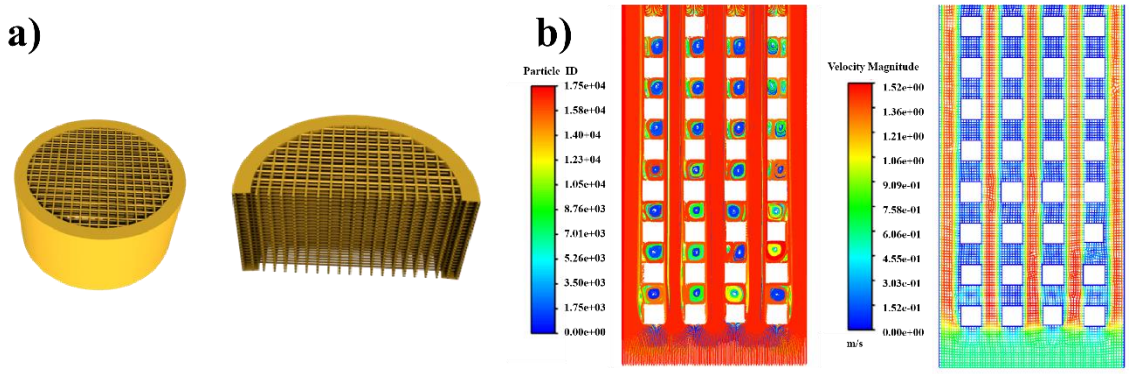

Figure S1. Three-Dimensional structural design and computational fluid dynamics (CFD) simulation of the 3D-printed integral adsorbent: **(a)** 3D structural schematic diagram; **(b)** CFD schematic diagram of 3D-printed integral adsorbent.

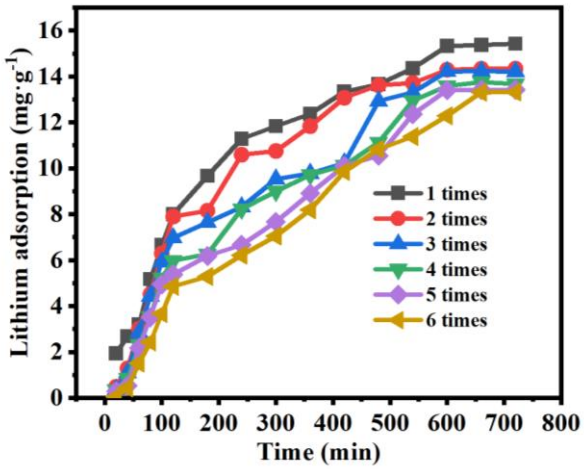

Figure S2. Fixed-bed adsorption stability.

	Powder	Granulation	DLP-0/DIW-1	Langmuir	Initial Concentration	Flow Velocity	Height	Diameter	Needle Diameter	Packing Density	Time	Ct/C0	Class
$Li_4Ti_5O_{12}$ + Montmorillonite	0	0	1	0.0176	100	1	6	1	0.26	0.15	20	0.013714	1
Activated carbon adsorption of dyes	1	0	0	0.114	0	100	0.5	6	10	0	1	30	2
GO adsorbs Cd	0	0	1	2.2861	1	0.5	0.2	24	14.5	0.5	0.5	100	3
Cellulose adsorption	0	0	1	0.013	1	15	15	2	15	1.4	0.3	20	4
Adsorption of copper	1	0	0	0.012	0	32	1.1	10	5	0	1	10	1
One-hot Code				Direct Input									Serial Number Coding

Matrix Merging

One-dimensional vector[0 0 1 1 0.0176 100 1 1 6 1 0.2 6 0.1520 0.13714 1]

Figure S3. Coding scheme.

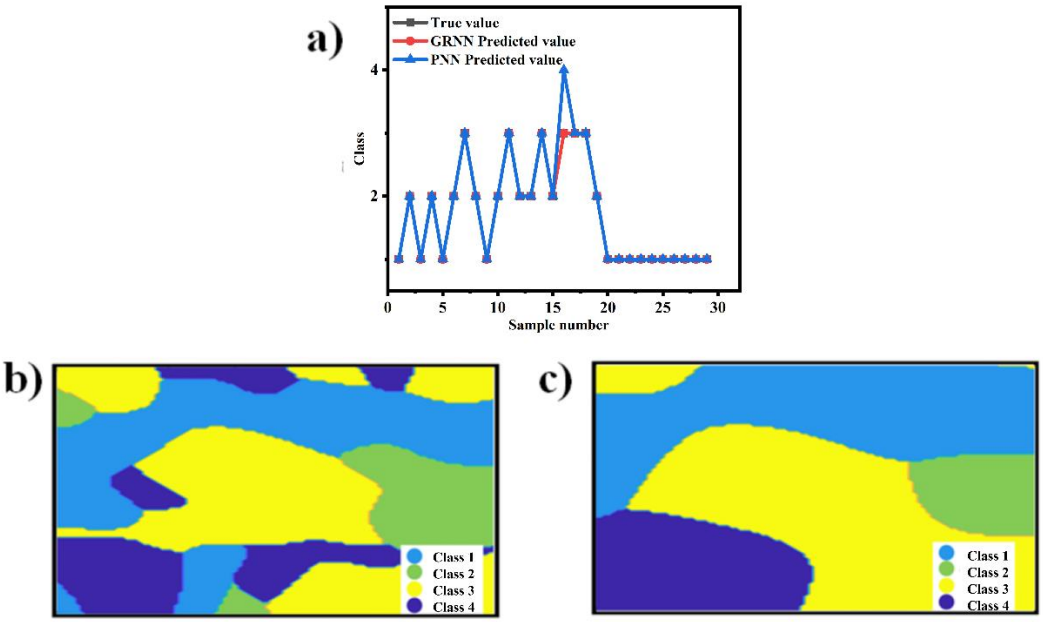

Figure S4. Comparison of classification performance across different models: **(a)** The calculation accuracy of PNN and GRNN; **(b)** Classification boundary of PNN; **(c)** Classification boundary of GRNN.

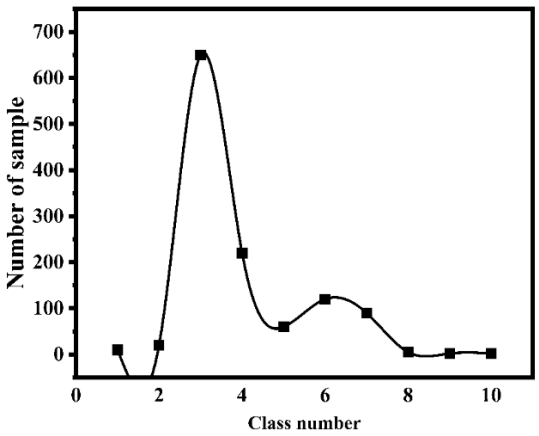

Figure S5. Sample distribution of CNN classification results.

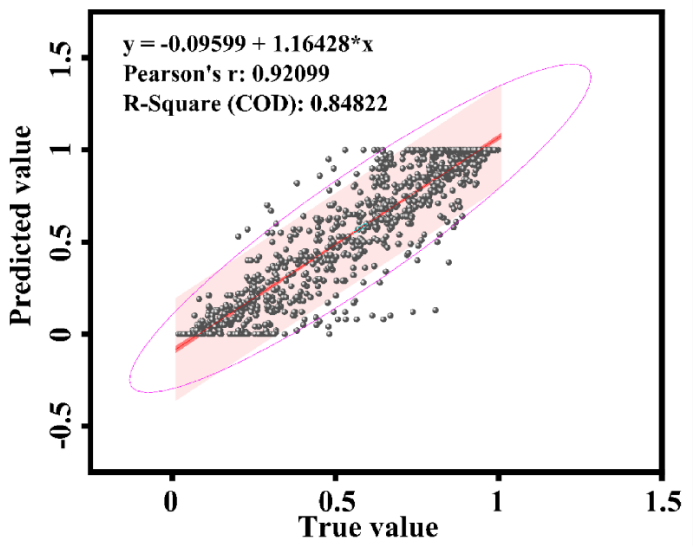

Figure S6. Linear regression diagram of random forest.

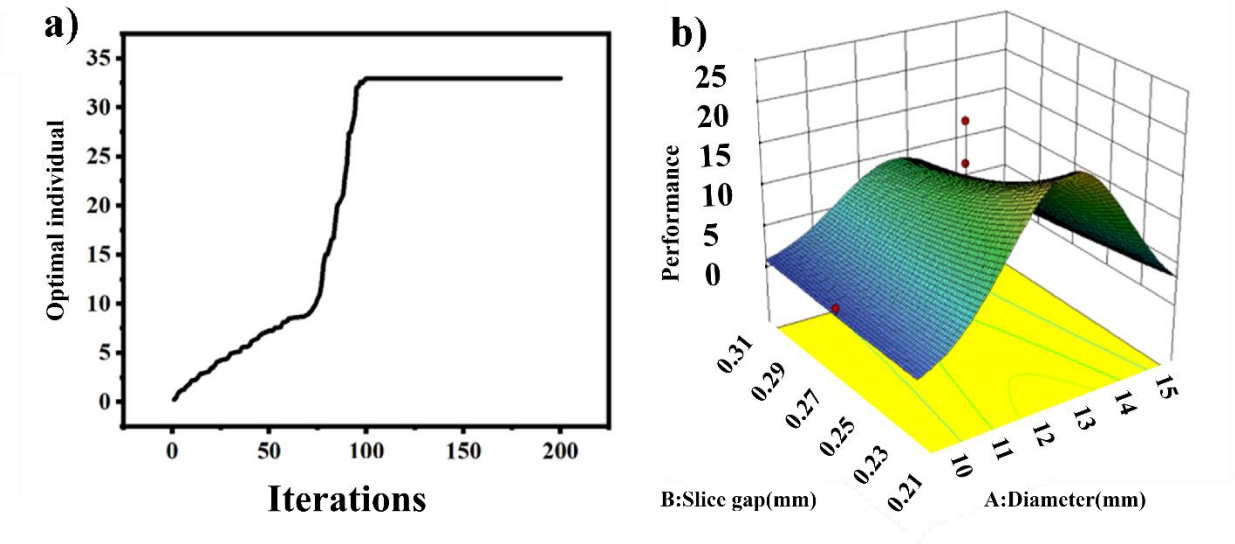

Figure S7. Optimal condition screening of genetic algorithm and response surface method: **(a)** Fitness variation diagram of genetic algorithm; **(b)** The best surface obtained by RSM.

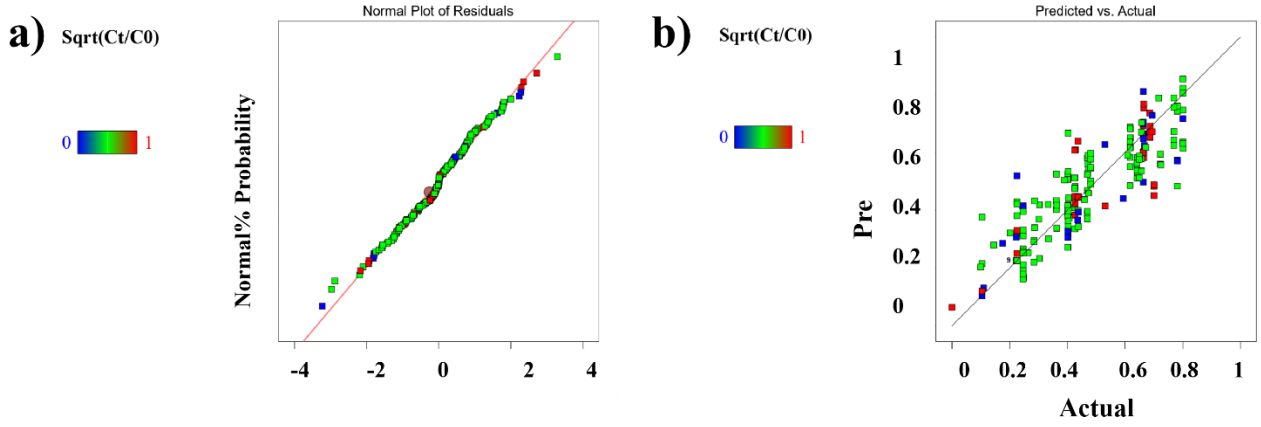

Figure S8. The accuracy of response surface method: **(a)** Linear regression diagram of predicted value and actual value; **(b)** Normal distribution of residuals.

2. Supplementary tables

Table S1. Variance analysis of quadratic meta-model of response surface.

Source	Sum of Squares	df	Mean Square	F-value	p-value	
Model	5.8000	90.000	0.0644	3.8200	< 0.0001	significant
A-Langmuir constant	0.0775	1.0000	0.0775	4.6000	0.0341	-
B-Powder	0.0001	1.0000	0.0001	0.0034	0.9537	-
C-Granulation	0.0031	1.0000	0.0031	0.1864	0.6667	-
D-3D Printing	0.0001	1.0000	0.0001	0.0046	0.9459	-
E-DLP-0/DIW-1	0.0067	1.0000	0.0067	0.3996	0.5286	-
F-initial concentration	0.0583	1.0000	0.0583	3.4600	0.0653	-
G-flow rate	0.0013	1.0000	0.0013	0.0798	0.7780	-
H-Bed height	0.0039	1.0000	0.0039	0.2342	0.6294	-
J-Packing diameter	0.0418	1.0000	0.0418	2.4800	0.1180	-
K-printing needle	0.0184	1.0000	0.0184	1.0900	0.2988	-
L-Packing density	0.3074	1.0000	0.3074	18.250	< 0.0001	-
M-Adsorption time	0.4577	1.0000	0.4577	27.170	< 0.0001	-
AB	0.0026	1.0000	0.0026	0.1559	0.6937	-
AC	0.0057	1.0000	0.0057	0.3363	0.5631	-
AD	0.0145	1.0000	0.0145	0.8628	0.3549	-
AE	0.0013	1.0000	0.0013	0.0795	0.7785	-
AF	0.0517	1.0000	0.0517	3.0700	0.0826	-
AG	0.0055	1.0000	0.0055	0.3273	0.5684	-
AH	0.0043	1.0000	0.0043	0.2541	0.6152	-
AJ	0.0036	1.0000	0.0036	0.2112	0.6467	-
AK	0.0036	1.0000	0.0036	0.2166	0.6425	-
AL	0.2502	1.0000	0.2502	14.850	0.0002	-
AM	0.0008	1.0000	0.0008	0.0479	0.8271	-
BC	0.0028	1.0000	0.0028	0.1668	0.6838	-
BD	0.0155	1.0000	0.0155	0.9227	0.3388	-
BE	0.0014	1.0000	0.0014	0.0844	0.7720	-
BF	0.0057	1.0000	0.0057	0.3406	0.5606	-
BG	0.0027	1.0000	0.0027	0.1589	0.6909	-
BH	0.0032	1.0000	0.0032	0.1896	0.6641	-
BJ	0.0016	1.0000	0.0016	0.0947	0.7589	-
BK	0.0155	1.0000	0.0155	0.9224	0.3389	-
BL	0.0218	1.0000	0.0218	1.3000	0.2575	-
BM	0.0666	1.0000	0.0666	3.9600	0.0491	-
CD	0.0001	1.0000	0.0001	0.0054	0.9415	-
CE	0.0008	1.0000	0.0008	0.0468	0.8292	-
CF	0.0020	1.0000	0.0020	0.1216	0.7279	-
CG	0.0002	1.0000	0.0002	0.0096	0.9222	-
CH	0.0056	1.0000	0.0056	0.3350	0.5639	-
CJ	0.0003	1.0000	0.0003	0.0196	0.8888	-
CK	0.0000	1.0000	0.0000	0.0017	0.9672	-
CL	0.0010	1.0000	0.0010	0.0570	0.8117	-
CM	0.0006	1.0000	0.0006	0.0352	0.8515	-
DE	0.2044	1.0000	0.2044	12.130	0.0007	-
DF	0.0165	1.0000	0.0165	0.9794	0.3245	-
DG	0.0408	1.0000	0.0408	2.4200	0.1226	-
DH	0.0013	1.0000	0.0013	0.0761	0.7832	-
DJ	0.0466	1.0000	0.0466	2.7600	0.0992	-
DK	0.0005	1.0000	0.0005	0.0280	0.8673	-
DL	0.0159	1.0000	0.0159	0.9461	0.3328	-
DM	0.0074	1.0000	0.0074	0.4366	0.5101	-
EF	0.0085	1.0000	0.0085	0.5052	0.4787	-
EG	0.0015	1.0000	0.0015	0.0872	0.7683	-
EH	0.0014	1.0000	0.0014	0.0832	0.7735	-
EJ	0.0058	1.0000	0.0058	0.3464	0.5573	-
EK	0.0004	1.0000	0.0004	0.0261	0.8719	-

Table S1. *Cont.*

Source	Sum of Squares	df	Mean Square	F-value	p-value	
EL	0.0248	1.0000	0.0248	1.4700	0.2274	-
EM	0.0410	1.0000	0.0410	2.4300	0.1216	-
FG	0.0082	1.0000	0.0082	0.4858	0.4872	-
FH	0.0029	1.0000	0.0029	0.1707	0.6803	-
FJ	0.0060	1.0000	0.0060	0.3567	0.5515	-
FK	0.0108	1.0000	0.0108	0.6407	0.4251	-
FL	0.0060	1.0000	0.0060	0.3567	0.5515	-
FM	0.1069	1.0000	0.1069	6.3400	0.0132	-
GH	0.0002	1.0000	0.0002	0.0112	0.9158	-
GJ	0.0471	1.0000	0.0471	2.8000	0.0972	-
GK	0.0261	1.0000	0.0261	1.5500	0.2156	-
GL	0.0005	1.0000	0.0005	0.0312	0.8602	-
GM	0.0037	1.0000	0.0037	0.2202	0.6398	-
HJ	0.0015	1.0000	0.0015	0.0917	0.7625	-
HK	0.0111	1.0000	0.0111	0.6601	0.4182	-
HL	0.0002	1.0000	0.0002	0.0102	0.9197	-
HM	0.0663	1.0000	0.0663	3.9400	0.0497	-
JK	0.0014	1.0000	0.0014	0.0819	0.7753	-
JL	0.0039	1.0000	0.0039	0.2312	0.6315	-
JM	0.0133	1.0000	0.0133	0.7915	0.3755	-
KL	0.1489	1.0000	0.1489	8.8400	0.0036	-
KM	0.0429	1.0000	0.0429	2.5500	0.1132	-
LM	0.2717	1.0000	0.2717	16.130	0.0001	-
A^2	0.2372	1.0000	0.2372	14.080	0.0003	-
B^2	0.0305	1.0000	0.0305	1.8100	0.1809	-
C^2	0.0019	1.0000	0.0019	0.1131	0.7373	-
D^2	0.1140	1.0000	0.1140	6.7700	0.0105	-
E^2	0.0579	1.0000	0.0579	3.4400	0.0664	-
F^2	0.0328	1.0000	0.0328	1.9500	0.1656	-
G^2	0.0283	1.0000	0.0283	1.6800	0.1974	-
H^2	1.1000	1.0000	1.1000	65.170	< 0.001	-
J^2	1.5000	1.0000	1.5000	89.220	< 0.001	-
K^2	0.1622	1.0000	0.1622	9.6300	0.0024	-
L^2	0.8077	1.0000	0.8077	47.950	< 0.001	-
M^2	0.0126	1.0000	0.0126	0.7455	0.38970	-
Residual	1.9000	1.0000	0.0168	-	-	-
Lack of Fit	1.9000	102.00	0.0187	18430.6	< 0.0001	significant
Pure Error	0.0000	11.00	1.013E-06	-	-	-
Cor Total	7.7000	203.00	-	-	-	-

Table S2. Different calculation errors of RBF neural network.

Algorithm	Transfer function for hidden layer	Transfer function for output layer	R^2	MSE
trainlm	tansig	purelin	0.990	0.008
	logsig		0.910	0.260
trainscg	tansig	purelin	0.960	0.024
	logsig		0.930	0.079
trainoss	tansig	purelin	0.830	0.250
	logsig		0.950	0.018
traingdm	tansig	purelin	0.910	0.249
	logsig		0.850	0.360
traingda	tansig	purelin	0.870	0.270
	logsig		0.970	0.021
trainr	tansig	purelin	0.950	0.012
	logsig		0.930	0.014